

1 **Evolutionary trajectories of snake genes and genomes revealed by comparative**
2 **analyses of five-pacer viper**

3 Wei Yin^{1,*}, Zong-ji Wang^{2,3,4,5,*}, Qi-ye Li^{3,4,6}, Jin-ming Lian³, Yang Zhou³, Bing-zheng
4 Lu⁷, Li-jun Jin³, Peng-xin Qiu⁷, Pei Zhang³, Wen-bo Zhu⁷, Bo Wen⁸, Yi-jun Huang⁷,
5 Zhi-long Lin⁸, Bi-tao Qiu^{3,9}, Xing-wen Su⁷, Huan-ming Yang^{8,9}, Guo-jie Zhang^{3,4,10},
6 Guang-mei Yan^{7,#}, Qi Zhou^{2,11,#}

7

8 1. Department of Biochemistry, Zhongshan School of Medicine, Sun Yat-sen University,
9 Guangzhou, 510089, China.

10 2. Life Sciences Institute, The Key Laboratory of Conservation Biology for Endangered
11 Wildlife of the Ministry of Education, Zhejiang University, Hangzhou, 310058,
12 China.

13 3. China National Genebank, BGI-Shenzhen, Shenzhen, 518083, China.

14 4. State Key Laboratory of Genetic Resources and Evolution, Kunming Institute of
15 Zoology, Chinese Academy of Sciences, Kunming, China.

16 5. School of Bioscience & Bioengineering, South China University of Technology,
17 Guangzhou, 510006, China.

18 6. Centre for GeoGenetics, Natural History Museum of Denmark, University of
19 Copenhagen, Øster Voldgade 5–7, 1350 Copenhagen K, Denmark.

20 7. Department of Pharmacology, Zhongshan School of Medicine, Sun Yat-sen
21 University, Guangzhou, 510089, China.

22 8. BGI-Shenzhen, Shenzhen, 518083, China.

23 9. James D. Watson Institute of Genome Sciences, Hangzhou 310058, China

24 10. Centre for Social Evolution, Department of Biology, University of Copenhagen,
25 Universitetsparken 15, DK-2100 Copenhagen, Denmark.

26 11. Department of Integrative Biology, University of California, Berkeley, Berkeley,
27 CA94720, United States

28 * These authors contributed equally to the work

29 # To whom correspondence should be addressed: zhouqi1982@zju.edu.cn or
30 ygm@mail.sysu.edu.cn

31 **Abstract**

32 Snakes have numerous features distinctive from other tetrapods and a rich history of
33 genome evolution that is still obscure. Here, we report the genome of the five-pacer viper,
34 *Deinagkistrodon acutus*, and comparative analyses with species from other major snake
35 and lizard lineages. We map the evolutionary trajectories of transposable elements (TEs),
36 developmental genes and sex chromosomes onto the snake phylogeny. TEs exhibit
37 dynamic lineage-specific expansion; in the viper, many TEs may have been rewired into
38 the regulatory network of brain genes. We detect signatures of adaptive evolution in
39 olfactory, venom and thermal-sensing genes, and also functional degeneration of genes
40 associated with vision and hearing. Many *Hox* and *Tbx* limb-patterning genes show
41 evidence of relaxed selective constraints, and their phylogenetic distribution supports
42 fossil evidence for a successive loss of forelimbs then hindlimbs during snake evolution.
43 Finally, we infer that the Z and W sex chromosomes had undergone at least three
44 recombination suppression events in the ancestor of advanced snakes, with the W
45 chromosomes showing a gradient of degeneration from basal to advanced snakes. These
46 results forge a framework for our deep understanding into snakes' history of molecular
47 evolution.

48 **Introduction**

49 Snakes have undergone a massive adaptive radiation with ~3400 extant species
50 successfully inhabiting almost all continents except for the polar regions¹. This process
51 has culminated in ‘advanced snakes’ (Caenophidia, ~3000 species), involved numerous
52 evolutionary changes in body form, chemo- and thermo-perception, venom and sexual
53 reproductive systems, which together distinguish snakes from the majority of other
54 squamates (lizards and worm lizards). Some of these dramatic changes can be tracked
55 from fossils, which have established that the ancestor of snakes had already evolved an
56 elongated body plan, probably as an adaptation to a burrowing and crawling lifestyle, but
57 had lost only the forelimbs²⁻⁴. Extant boa and python species retain rudimentary
58 hindlimbs, whereas advanced snakes have completely lost them. Limblessness,
59 accompanied by degeneration in visual and auditory perception, has not compromised
60 snakes’ dominant role as top predators, largely due to the evolution of infrared sensing
61 and/or venom, and the development of corresponding facial pit and fangs (specialized
62 teeth for venom injection) independently in different lineages^{5,6}.

63 These extreme adaptations have sparked strong and standing interest into their
64 genetic basis. Snakes are used as a model for studying various basic questions about the
65 mechanisms of axial patterning and limb development^{3,7,8}, ‘birth-and-death’ of venom
66 proteins⁹⁻¹¹, and sex chromosome evolution¹². Cytogenetic findings in snakes first drove
67 Ohno to propose that sex chromosomes in vertebrates evolved from ancestral
68 autosomes¹³, such as those of insects¹⁴ and plants¹⁵. Insights into these questions have
69 been advanced recently by the application of next-generation sequencing. Analyses of
70 python and king cobra genomes and transcriptomes have uncovered the metabolic gene
71 repertoire involved in feeding, and inferred massive expansion and adaptive evolution of
72 toxin families in elapids (an ‘advanced’ group)^{10,16}. However, comparative studies of
73 multiple snake genomes unraveling their evolutionary trajectories since the divergence
74 from lizards are lacking, and so far only a few specific developmental ‘toolbox’ (e.g.,
75 *Hox*^{7,17,18} and Fgf signaling pathway¹⁹) genes have been studied between snakes and
76 lizards. This hampers our comprehensive understanding into the molecular basis of
77 stepwise or independent acquisition of snake-specific traits. We bridge this gap here by

78 deep-sequencing the genomes and transcriptomes of the five-pacer viper,
79 *Deinagkistrodon acutus* (**Figure 1A**), a member of the Viperidae family. This pit viper is
80 a paragon of infrared sensing, heteromorphic ZW sex chromosomes, and distinctive types
81 of fangs and toxins (its common name exaggerates that victims can walk no more than
82 five paces) from other venomous snake families^{6,20}. Despite the intraspecific differences
83 within the same family, comparative analyses to the available genomes of three other
84 major snake family species, i.e., *Boa constrictor* (Boidae family)²¹, *Python bivittatus*
85 (Pythonidae family)¹⁶, *Ophiophagus hannah* (Elapidae family)¹⁰ and several reptile
86 outgroups should recapitulate the major genomic adaptive or degenerative changes that
87 occurred in the ancestor and along individual branches of snake families, and would also
88 promote current antivenom therapy and drug discovery (e.g., thrombolytics) out of the
89 viper toxins²².

90

91

92 **Results**

93 **Evolution of snake genome architecture**

94 We sequenced a male and a female five-pacer viper (*Deinagkistrodon acutus*) to
95 high-coverage (♀ 238 fold, ♂ 114 fold, **Supplementary Table 1**), and estimated the
96 genome size to be 1.43Gb based on k-mer frequency distribution²³ (**Supplementary**
97 **Table 2, Supplementary Figure 1**). Fewer than 10% of the reads, which have a low
98 quality or are probably derived from repetitive regions, were excluded from the genome
99 assembly (**Supplementary Table 3**). We generated a draft genome using only male reads
100 for constructing the contigs, and female long-insert (2kb~40kb) library reads for joining
101 the contigs into scaffolds. The draft genome has an assembled size of 1.47Gb, with a
102 slightly better quality than the genome assembled using only female reads. The draft
103 genome has high continuity (contig N50: 22.42kb, scaffold N50: 2.12Mb) and integrity
104 (gap content 5.6%, **Supplementary Table 4**), and thus was chosen as the reference
105 genome for further analyses. It includes a total of 21,194 predicted protein-coding genes,
106 as estimated using known vertebrate protein sequences and transcriptome data generated
107 in this study from eight tissues (**Figure 1A, Methods**). For comparative analyses, we also

108 annotated 17,392 protein-coding genes in the boa genome (the SGA version from²¹).
109 80.84% (17,134) of the viper genes show robust expression (normalized expression level
110 RPKM>1) in at least one tissue, comparable to 70.77% in king cobra (**Supplementary**
111 **Table 5**). Based on 5,353 one-to-one orthologous gene groups of four snake species
112 (five-pacer viper, boa²¹, python¹⁶, king cobra¹⁰), the green anole lizard²⁴ and several other
113 sequenced vertebrate genomes (**Methods**), we constructed a phylogenomic tree with high
114 bootstrapping values at all nodes (**Figure 1B**). We estimated that advanced snakes
115 diverged from boa and python about 66.9 (47.2~84.4) million years ago (MYA), and
116 five-pacer viper and king cobra diverged 44.9 (27.5~65.0) MYA assuming a molecular
117 clock. These results are consistent with the oldest snake and viper fossils from 140.8 and
118 84.7 MYA, respectively²⁵.

119 The local GC content of snakes (boa and five-pacer viper) shows variation (GC
120 isochores) similar to the genomes of turtles and crocodiles, and intermediate between
121 mammals/birds and lizard (**Figure 1C, Supplementary Figure 2**), confirming the loss of
122 such a genomic feature in lizard²⁴. Cytogenetic studies showed that, like most other
123 snakes, the five-pacer viper karyotype has 2n=36 chromosomes (16 macro- and 20
124 micro-chromosomes)²⁶, with extensive inter-chromosomal conservation with the lizard²⁷.
125 This enables us to organize 56.50% of the viper scaffold sequences into linkage groups,
126 based on their homology with sequences of known green anole lizard
127 macro-chromosomes (**Supplementary Table 6**). As expected, autosomal sequences have
128 the same read coverage in both sexes, whereas scaffolds inferred to be located on the
129 viper Z chromosome (homologous to green anole lizard chr6) have coverage in the
130 female that is half that in the male (**Figure 1C**). Additionally, the frequency of
131 heterozygous variants on the Z chromosome is much lower in the female than in the male
132 (0.005% vs 0.08%, Wilcoxon signed rank test, P -value<2.2e-16,) due to the nearly
133 hemizygous state of Z chromosome in female, while those of autosomes (~0.1%) are very
134 similar between sexes. These results indicate that our assembly mostly assigns genes to
135 the correct chromosome, and correct chromosome assignment is further supported by
136 comparison of 172 genes' locations with previous fluorescence *in situ* hybridization
137 results (**Supplementary Data 1**)²⁷. They also suggest that the viper sex chromosomes are

138 highly differentiated from each other (see below).

139 47.47% of the viper genome consists of transposable element sequences (TEs), a
140 higher percentage than in any other snake so far analyzed (33.95~39.59%), which cannot
141 be explained solely by the higher assembly quality here^{10,16,21} (**Supplementary Table**
142 **7-8**). The TEs in the viper genome are mostly long interspersed elements (LINE, 13.84%
143 of the genome) and DNA transposons (7.96%, **Supplementary Table 7**). Sequence
144 divergence of individual families from inferred consensus sequences uncovered recent
145 rampant activities in the viper lineage of LINEs (CR1), DNA transposons (hAT and
146 TcMar) and retrotransposons (Gypsy and DIRS). In particular, there is an excess of
147 low-divergence (<10% divergence level) CR1 and hAT elements in the viper genome
148 only (**Figure 2A**). We also inferred earlier propagation of TEs shared by viper and king
149 cobra, which thus probably occurred in the ancestor of advanced snakes. Together, these
150 derived insertions resulted in an at least three-fold difference in the CR1 and hAT content
151 between viper and more basal-branching snakes such as the boa and python (**Figure 2B**).
152 Meanwhile, the boa and python have undergone independent expansion of L2 and CR1
153 repeats, so that their overall LINE content is at a similar level to that of the viper and
154 cobra (**Figure 2A, Supplementary Table 7**).

155 These TEs are presumably silenced through epigenetic mechanisms to prevent their
156 deleterious effects of transposition and mediation of genomic rearrangements. Indeed,
157 very few TEs are transcribed in all of the tissues examined, except, unexpectedly, in the
158 brain (**Figure 2C**). This brain-specific expression prompted us to test whether some
159 snake TE families might have been co-opted into brain gene regulatory networks.
160 Focusing on highly expressed (RPKM>5) TEs that are located within 5kb flanking
161 regions of genes, we found that these nearby genes also show a significantly higher
162 expression in brain than in any other tissues (Wilcoxon test, P -value<1.1e-40,
163 **Supplementary Figure 3**). The expression levels of individual genes are strongly
164 correlated (Spearman's test, P -value<1.35e-08) with those of nearby TEs. These genes
165 are predominantly enriched (Fisher's Chi-square test, Q -value < 0.05, **Supplementary**
166 **Data 2**) in functional domains of 'biological process' compared to 'cellular component'
167 and 'molecular function', and particularly enriched categories include environmental

168 response ('response to organic substance', 'regulation of response to stimulus' and
169 'sensory perception of light stimulus') and brain signaling pathways ('neuropeptide
170 signaling pathway', 'opioid receptor signaling pathway' and 'regulation of cell
171 communication' etc.). Further experimental studies are required to elucidate how some of
172 these TEs evolved to regulate gene expression in the brain; these results nevertheless
173 highlight the evolutionary dynamics and potential functional contribution of TEs in
174 shaping snake genome evolution.

175

176 **Evolution of snake genes and gene families**

177 To pinpoint the critical genetic changes underlying the phenotypic innovations of snakes,
178 we next mapped protein coding genes' gain and loss (**Figure 1B**), signatures of adaptive
179 or degenerative evolution (**Figure 3A**) measured by their ratios (ω) of nonsynonymous vs.
180 synonymous substitution rates (**Supplementary Data 3**) onto the phylogenetic tree. We
181 inferred a total of 1,725 gene family expansion and 3,320 contraction events, and
182 identified 610 genes that appear to have undergone positive selection and 6149 with
183 relaxed selective constraints at different branches, using a likelihood model and
184 conserved lineage-specific test²⁸. Genes of either scenario were separated for analysis of
185 their enriched gene ontology (GO) and mouse orthologs' mutant phenotype terms,
186 assuming most of them have a similar function in snakes.

187 Significantly (Fisher's exact test, P -value<0.05) enriched mutant phenotype terms
188 integrated with their branch information illuminated the molecular evolution history of
189 snake-specific traits (**Figure 3A**). For example, as adaptations to a fossorial lifestyle, the
190 four-legged snake ancestor²⁹ had evolved an extreme elongated body plan without limbs,
191 and also fused eyelids ('spectacles', presumably for protecting eyes against soil³⁰). The
192 latter is supported by the results for the positively selected gene *Ereg* and the genes under
193 relaxed selection *Cecr2* and *Ext1* at the snake ancestor branch (**Supplementary Data 4**),
194 whose mouse mutant phenotype is shown as prematurely opened or absent eyelids. The
195 limbless body plan has already driven many comparisons of expression domains and
196 coding-sequences of the responsible *Hox* genes between snakes and other vertebrates^{7,17}.
197 We here refined the analyses to within snake lineages, focusing on sequence evolution of

198 *Hox* and other genes involved in limb development and somitogenesis. We annotated the
199 nearly complete sequences of 39 *Hox* genes organized in four clusters (*HoxA-HoxD*) of
200 the five-pacer viper. Compared to the green anole lizard, the four studied snake species
201 have *Hox* genes whose sizes are generally reduced, due to the specific accumulation of
202 DNA transposons in the lizard's introns and intergenic regions (**Supplementary Figure**
203 **4**). However, snakes have accumulated particularly higher proportions of simple tandem
204 repeat and short interspersed element (SINE) sequences within *Hox* clusters
205 (**Supplementary Figure 5**), either as a result of relaxed selective constraints and/or
206 evolution of novel regulatory elements. We identified 11 *Hox* genes as under relaxed
207 selective constraint and one (*Hoxa9*) as under positive selection (**Figure 3B**). Their
208 combined information of gene function and affected snake lineage informed the stepwise
209 evolution of snake body plan. In particular, *Hoxa5*³¹, *Hoxa11*³² and *Tbx5*³³, which
210 specifically pattern the forelimbs in mouse, have been identified as genes under relaxed
211 selective constraint in the common ancestor of all four snakes. Meanwhile, *Hoxc11* and
212 *Tbx4*³⁴, which pattern the hindlimbs in the mouse, and many other limb-patterning genes
213 (e.g. *Gli3*, *Tbx18*, *Alx4*) were identified as genes under relaxed selective constraint that
214 evolved independently on snake external branches (**Figure 3B, Supplementary Data 4**).
215 These results provide robust molecular evidence supporting the independent loss of
216 hindlimbs after the complete loss of forelimbs in snake ancestors. In the snake ancestor
217 branch, we also identified the genes under relaxed selective constraint *Hoxa11*, *Hoxc10*
218 and *Lfng*, which are respectively associated with sacral formation³⁵, rib formation⁸ and
219 somitogenesis speed³⁶ in vertebrates. Their changed amino acids and the expression
220 domains that have expanded in snakes relative to lizards^{17,19} might have together
221 contributed to the 'de-regionalization'¹⁷ and elongation of the snake body plan. In several
222 external branches, we identified *Hoxd13* independently as under relaxed selective
223 constraint. Besides its critical roles in limb/digit patterning³⁷, *Hoxd13* is also associated
224 with termination of the somitogenesis signal and is specifically silenced at the snake tail
225 relative to lizard⁷. This finding suggests that body elongation may have evolved more
226 than once among snake lineages. Overall, limb/digit/tail development mutant phenotype
227 terms are significantly enriched in genes under relaxed selective constraint at both

228 ancestral and external branches of snakes (**Figure 3A**), and we identified many such
229 genes in different snake lineages for future targeted experimental studies
230 (**Supplementary Table 9, Supplementary Data 4**).

231 Another important adaption to the snakes' ancestrally fossorial and later ground
232 surface lifestyle is the shift of their dominant source of environmental sensing from
233 visual/auditory to thermal/chemical cues. Unlike most other amniotes, extant snake
234 species do not have external ears, and some basal species (e.g., blindsnake) have
235 completely lost their eyes. Consistently, we found mutant phenotype terms associated
236 with hearing/ear and vision/eye phenotypes (e.g., abnormal ear morphology, abnormal
237 vision, abnormal cone electrophysiology) are enriched among genes under relaxed
238 selection along all major branches of snakes starting from their common ancestor (**Figure**
239 **3A, Supplementary Figure 6, Supplementary Data 4**). Gene families that have
240 contracted in the ancestor of the four studied snake species, and specifically in the viper,
241 are also significantly enriched in gene ontologies (GO) of 'sensory perception of light
242 stimulus (GO:0050953)' or 'phototransduction (GO:0007602)' (Fisher's Exact Test,
243 $Q\text{-value} < 9.08\text{e-}4$; **Figure 1C, Supplementary Data 5**). In particular, only three (*RHI*,
244 *LWS* and *SWS1*) out of 13 opsin genes' complete sequences can be identified in the viper
245 genome, consistent with the results found in python and cobra¹⁶. By contrast, infrared
246 receptor gene *TRPA1*⁵ and ubiquitous taste-signaling gene *TRPM5*³⁸ have respectively
247 undergone adaptive evolution in five-pacer viper and the ancestor of boa and python.
248 Gene families annotated with the GO term 'olfactory receptor (OR) activity' have a
249 significant expansion in all snake species studied (Fisher's Exact Test, $Q\text{-value} < 1.63\text{e-}4$)
250 and at some of their ancestral nodes, except for the king cobra (**Supplementary Data 6**).
251 In the boa and viper, whose genome sequences have much better quality than the other
252 two snake genomes, we respectively annotated 369 and 412 putatively functional OR
253 genes, based on homology search and the characteristic 7-TM (transmembrane) structure
254 (**Methods**). Both terrestrial species have an OR repertoire predominantly comprised of
255 class II OR families (OR1-14, presumably for binding airborne molecules, **Figure 3C**),
256 and their numbers are much higher than the reported numbers in other squamate
257 genomes³⁹. Some (ranging from 18 to 24) class I (OR51-56, for water-borne molecules)

258 genes have also been found in the two species, indicating this OR class is not unique to
259 python as previously suggested³⁹. Compared with the green anole lizard, the boa and
260 viper exhibit a significant size expansion of OR family 5, 11 and 14 (Fisher's exact test
261 $P < 0.05$), and also a bias towards being located on the Z chromosome (**Figure 3C**),
262 leading to higher expression of many OR genes in males than in females (see below). In
263 particular, OR5 in the viper probably has experienced additional expansion events and
264 become the most abundant (with 71 members) family in the genome. Intriguingly, this
265 family is specifically enriched in birds of prey⁴⁰ relative to other birds, and in
266 non-frugivorous bats vs. frugivorous bats⁴¹. Therefore, its expansion in the five-pacer
267 viper could have been positively selected for a more efficient detection of prey.

268 Besides acute environmental sensing, specialized fangs⁶ and venoms¹¹ (e.g.,
269 hemotoxins of viper or neurotoxins of elapid) arm the venomous snakes (~650 species) to
270 immediately immobilize much larger prey for prolonged ingestion, which probably
271 comprised one of the most critical factors that led to the advanced snakes' species
272 radiation. It has been proposed that the tremendous venom diversity probably reflects
273 snakes' local adaption to prey⁴² and was generated by changes in the expression of
274 pre-existing or duplicated genes^{11,43}. Indeed, we found that the five-pacer viper's venom
275 gland gene repertoire has a very different composition compared to other viper⁴⁴ or elapid
276 species¹⁰ (**Figure 3D**). We have annotated a total of 35 venom genes or gene families
277 using all the known snake venom proteins as the query. Certain gene families, including
278 snake venom metalloproteinases (SVMP), C-type lectin-like proteins (CLPs),
279 thrombin-like snake venom serine proteinases (TL), Kunitz and disintegrins, have more
280 genomic copies in the five-pacer viper than other studied snakes or the green anole lizard
281 (**Supplementary Table 10**), whereas characteristic elapid venom genes such as
282 three-finger toxins (3FTx) are absent from the viper genome. Most venom proteins of
283 both the viper and king cobra have expression restricted to venom or accessory glands,
284 and for both species this is particularly seen for those genes that originated in the ancestor
285 of snakes or of advanced snakes (**Figure 3D**). However, elapid- and viper-specific venom
286 genes, i.e., those that originated more recently, are usually expressed in the liver of the
287 other species. Such cases include FactorV, FactorX of king cobra and PLA2-2A of viper

288 **(Figure 3D)**. This expression pattern suggests that these venom genes may have
289 originated from metabolic proteins and undergone neo-/sub-functionalization, with
290 altered expression.

291

292 **Evolution of snake sex chromosomes**

293 Different snake species exhibit a continuum of sex chromosome differentiation. Pythons
294 and boas possess homomorphic sex chromosomes, which is assumed to be the ancestral
295 state; the lack of differentiation between the W and Z chromosomes in these species
296 suggests that most regions of this chromosome pair recombine like the autosomes⁴⁵.
297 Advanced snakes usually have heteromorphic sex chromosomes that have undergone
298 additional recombination suppression^{45,46}. We found that the five-pacer viper probably
299 has suppressed recombination throughout almost the entire sex chromosome pair, as the
300 read coverage in the female that we sequenced is half that in the male (**Figure 1C, Figure**
301 **4**). By contrast, the boa's homologous chromosomal regions show a read coverage pattern
302 that does not differ from that of autosomes. Assuming that these two species share the
303 same ancestral snake sex-determining region, this suggests that that region is not included
304 in our current chromosomal assembly.

305 In plants, birds and mammals, it has been found that recombination suppression
306 probably occurred by a succession of events. This has led to the punctuated accumulation
307 of excessive neutral or deleterious mutations on the Y or W chromosome by genetic drift,
308 and produced a gradient of sequence divergence levels over time, which are termed
309 'evolutionary strata'⁴⁷⁻⁴⁹. Advanced snakes have been suggested to have at least two
310 strata¹². One goal of our genome assembly of the five-pacer viper compared to those of
311 any other studied advanced snakes^{10,12} (**Supplementary Table 4**) was to reconstruct a
312 fine history of snake sex chromosome evolution. We assembled 77Mb Z-linked and
313 33Mb W-linked scaffolds (**Methods**). The reduction of female read coverage along the Z
314 chromosome suggests that there is substantial divergence between Z- and W- linked
315 sequences; this divergence would enable the separate assembly of two chromosomes'
316 scaffolds. Mapping the male reads confirmed that the inferred W-linked scaffold
317 sequences are only present in the female (**Supplementary Figure 7**). Their density and

318 pairwise sequence divergence values within putative neutral regions along the Z
319 chromosome indicate at least two ‘evolutionary strata’, with the older stratum extending
320 0~56Mb, and the younger one extending 56~70Mb. The boundary at 56Mb region can
321 also be confirmed by analyses of repetitive elements on the Z chromosome (see below).
322 Consistently, identifiable W-linked fragments are found at the highest density per
323 megabase in the latter (**Figure 4**), suggesting that this recombination in this region has
324 been suppressed more recently. The older stratum includes much fewer identifiable
325 fragments that can resolve the actual times of recombination suppression events. To study
326 this region further, we inspected the homologous Z-linked region, whose recombination
327 has also been reduced, albeit to a much smaller degree than that of the W chromosome,
328 after the complete suppression of recombination between Z and W in females. In addition,
329 Z chromosome transmission is biased in males. As males usually have a higher mutation
330 rate than females, due to many more rounds of DNA replication during spermatogenesis
331 than during oogenesis (‘male-driven evolution’)⁵⁰, Z-linked regions are expected to have
332 a generally higher mutation rate than any other regions in the genome. This male-driven
333 evolution effect has been demonstrated in other snake species¹² and also been validated
334 for the snakes inspected in this study (**Supplementary Figure 8**). As a result, we
335 expected that regions in older strata should be more diverged from their boa
336 autosome-like homologs than those in the younger strata. This enabled us to identify
337 another stratum (0~42Mb, stratum 2, S2 in **Figure 4**) and demarcate the oldest one
338 (42~56Mb, S1), by estimating the sequence conservation level (measured by LASTZ
339 alignment score, blue line) between the Z chromosomes of boa and viper. The Z-linked
340 region in the inferred oldest stratum S1 exhibits the highest sequence divergence with the
341 homologous W-linked region and also the highest proportion of repetitive elements (CR1,
342 Gypsy and L1 elements; **Figure 4** shows the example of Gypsy; other repeats are shown
343 in **Supplementary Figure 9**). This can be explained by the effect of genetic drift⁵¹, which
344 has been acting on the Z-linked S1 for the longest time since it reduced recombination
345 rate in females. As a result, the accumulated repeats of S1 also tend to have a higher
346 divergence level from the inferred ancestral consensus sequences compared to nearby
347 strata (**Figure 4**). Unexpectedly, a similar enrichment was found in the homologous

348 region of S1 in boa, despite it being a recombining region and exhibiting the same
349 coverage depth between sexes (**Figure 4, Supplementary Figure 9**). This finding
350 indicates that the pattern is partially contributed by the ancestral repeats that had already
351 accumulated on the proto-sex chromosomes of snake species. Since our current viper sex
352 chromosomal sequences used the green anole lizard chromosome 6 as a reference,
353 rearrangements within this chromosome make it impossible to test whether S2
354 encompasses more than one stratum.

355 We dated the three resolved strata by constructing phylogenetic trees with
356 homologous Z- and W- linked gene sequences of multiple snake species. Combining the
357 published CDS sequences of pygmy rattlesnake (Viperidae family species) and garter
358 snake (Colubridae family species)¹², we found 31 homologous Z-W gene pairs,
359 representing the three strata. All of them clustered by chromosome (i.e., the Z-linked
360 sequences from all the species cluster together, separately from the W-linked ones) rather
361 than by species (**Supplementary Figure 10-12**). This clustering pattern indicates that all
362 three strata formed before the divergence of the advanced snakes and after their
363 divergence from boa and python, i.e., about 66.9 million years ago (**Figure 1C**).

364 We found robust evidence of functional degeneration on the W chromosome. It is
365 more susceptible to the invasion of TEs; the assembled sequences' overall repeat content
366 is at least 1.5 fold higher than that of the Z chromosome, especially in the LINE L1 (2.9
367 fold) and LTR Gypsy families (4.3 fold) (**Supplementary Table 11 and Supplementary**
368 **Figure 13**). Of 1,135 Z-linked genes, we were only able to identify 137 W-linked
369 homologs. Among these, 62 (45.26%) have probably become pseudogenes due to
370 nonsense mutations (**Supplementary Table 12**). W-linked loci generally are transcribed
371 at a significantly lower level (Wilcoxon test, P -value<0.0005), with pseudogenes
372 transcribed at an even lower level relative to the autosomal or Z-linked loci regardless of
373 the tissue type (**Supplementary Figure 14-15**). Given such a chromosome-wide gene
374 loss, as in other snakes¹² and the majority of species with ZW sex chromosomes⁵², the
375 five-pacer viper shows a generally male-biased gene expression throughout the
376 Z-chromosome and probably has not evolved global dosage compensation
377 (**Supplementary Figure 16**).

378

379 **Discussion**

380 The ‘snake-like’ body plan has evolved repeatedly in other tetrapods (e.g., worm lizard
381 and caecilians), in which limb reduction/loss seems to have always been accompanied by
382 body elongation. For example, several limb-patterning *Hox* genes (*Hoxc10*, *Hoxd13*)
383 identified as under relaxed selective constraints also have been characterized by previous
384 work with a changed expression domain along the snake body axis^{7,17}. Another gene
385 under relaxed selective constraint, *Hoxa5*, which is involved in the forelimb patterning³¹,
386 also participates in lung morphogenesis⁵³. *Hoxa5* might have been involved in the
387 elimination of one of the snake lungs during evolution. Therefore, the newly identified
388 genes under positive selection or under relaxed selective constraint throughout the snake
389 phylogeny in this work (**Supplementary Data 3-4, Supplementary Table 9**) can provide
390 informative clues for future experimental work to use the snake as an emerging ‘evo-devo’
391 model⁵⁴ to understand the genomic architecture of the developmental regulatory network
392 of organogenesis, or the crosstalk between these networks.

393 Like many of its reptile relatives, the snake ancestor is very likely to have determined
394 sex by temperature and to have lacked sex chromosomes. Extant species Boa can still
395 undergo occasional parthenogenesis and is able to produce viable WW offspring⁵⁵,
396 consistent with it having the most primitive vertebrate sex chromosome pair reported to
397 date. In the ancestor of advanced snakes, we inferred that there at least three
398 recombination suppression events occurred between Z and W, leading to the generally
399 degenerated W chromosome that we have observed in the five-pacer viper. How snakes
400 determine sex genetically is an intriguing question to study in the future.

401

402 **Methods**

403 **Genome sequencing and assembly**

404 All animal procedures were carried out with the approval of China National Genebank
405 animal ethics committee. We extracted genomic DNAs from blood of a male and a
406 female five-pacer viper separately. A total of 13 libraries with insert sizes ranging from
407 250bp to 40kb were constructed using female DNA, and three libraries with insert sizes

408 from 250 bp to 800 bp were constructed using male DNA. We performed paired-end
409 sequencing (HiSeq 2000 platform) following the manufacturer's protocol, and produced
410 528 Gb raw data (357 Gb for female and 171 Gb for male). We estimated the genome size
411 based on the K-mer distribution. A K-mer refers to an artificial sequence division of K
412 nucleotides iteratively from sequencing reads. The genome size can then be estimated
413 through the equation $G=K_num/Peak_depth$, where the K_num is the total number of
414 K-mer, and Peak_depth is the expected value of K-mer depth⁵⁶. We found a single main
415 peak in the male K-mer (K=17) frequency distribution and an additional minor peak in
416 the female data, the latter of which probably results from the divergence between W and
417 Z chromosomes (**Supplementary Figure 1**). Based on the distribution, we estimated that
418 the genome size of this species is about 1.43 Gb (**Supplementary Table 2**), comparable
419 to that of other snakes (1.44 Gb and 1.66Gb for Burmese python and King cobra^{10,16},
420 respectively).

421 After filtering out low-quality and duplicated reads, we performed additional filtering
422 using the following criteria: we excluded the reads from short-insert libraries (250, 500,
423 800 bp) with 'N's over 10% of the length or having more than 40 bases with the quality
424 lower than 7, and the reads from large-insert libraries (2 kb to 40 kb) with 'N's over 20%
425 of the length or having more than 30 bases with the quality lower than 7. Finally, 109.20
426 Gb (73X coverage) male reads and 148.49Gb (99X coverage) female reads were retained
427 for genome assembly (**Supplementary Table 1**) using SOAPdenovo⁵⁷
428 (<http://soap.genomics.org.cn>). To assemble the female and male genomes, reads from
429 small-insert libraries of the female and male individual were used for contig construction
430 separately. Then read-pairs from small- and large-insert libraries were utilized to join the
431 contigs into scaffolds. We also used female long-insert libraries to join the male contigs
432 into the longer scaffolds. At last, small-insert libraries of female and male individuals
433 were used for gap closure for their respective genomes. The final assemblies of female
434 and male have a scaffold N50 length of 2.0 Mb and 2.1 Mb respectively, and the gap
435 content of the two genomes are both less than 6% (♀ 5.29%, ♂ 5.61%)(**Supplementary**
436 **Table 4**).

437 To access the assembly quality, reads from small-insert libraries that passed our

438 filtering criteria were aligned onto the two assemblies using BWA⁵⁸ (Version: 0.5.9-r16)
439 allowing 8 mismatches and 1 indel per read. A total of ~97% reads can be mapped back
440 to the draft genome (**Supplementary Table 3**), spanning 98% of the assembled regions
441 excluding gaps (**Supplementary Table 13**), and most genomic bases were covered by
442 about 80X reads (**Supplementary Figure 17**). Thus, we conclude that we have
443 assembled most part of the five-pacer viper genome. To further test for potential
444 mis-joining of the contigs into scaffolds, we analyzed the paired-end information and
445 found that 57% of the paired-end reads can be aligned uniquely with the expected
446 orientation and distance. This proportion of the long insert library is significantly lower
447 than that from the short insert libraries due to a circulization step during the library
448 construction. When such paired-ends were excluded, the proportion increased to 94.98%
449 (**Supplementary Table 3**). Overall, these tests suggested that the contigs and scaffolds
450 are consistent with the extremely high density of paired-end reads, which in turn
451 indicated the high-quality of the assembly.

452 Previous cytogenetic studies showed that snake genomes show extensive
453 inter-chromosomal conservation with lizard^{27,45}. Thus, we used the chromosomal
454 information from green anole lizard²⁴ as a proxy to assign the snake scaffolds. We first
455 constructed their orthologous relationship combining information of synteny and
456 reciprocal best BLAST hits (RBH). Then gene coordinates and strandedness from the
457 consensus chromosome were used to place and orient the snake scaffolds. Furthermore,
458 we linked scaffolds into chromosomes with 600 'N's separating the adjacent scaffolds. In
459 total, 625 five-pacer viper scaffolds comprising 832Mb (56.50% scaffolds in length) were
460 anchored to 5 autosomes and Z chromosome (**Supplementary Table 6**).

461

462 **Repeat and gene annotation**

463 We identified the repetitive elements in the genome combining both homology-based and
464 *de novo* predictions. We utilized the 'Tetrapoda' repeat consensus library in Rebase⁵⁹ for
465 RepeatMasker (<http://www.repeatmasker.org>) to annotate all the known repetitive
466 elements in the five-pacer viper genome. In order to maximize the identification and

467 classification of repeat elements, we further used RepeatModeler
468 (<http://www.repeatmasker.org/RepeatModeler.html>) to construct the consensus repeat
469 sequence libraries of the green anole lizard, boa and five-pacer viper, then used them as a
470 query to identify repetitive elements using RepeatMasker. Finally, we retrieved a
471 non-redundant annotation for each species after combining all the annotation results
472 using libraries of ‘Tetrapoda’, ‘green anole lizard’, ‘boa’ and ‘five-pacer viper’. For the
473 purpose of comparison, we ran the same pipeline and parameters in all the snake and
474 lizard genomes as shown in **Supplementary Table 7**. To provide a baseline estimate for
475 the sequence divergence of TEs from the snake ancestral status, we first merged the
476 genomes from boa and five-pacer viper, and constructed the putative ancestral consensus
477 sequences using RepeatModeler. Then TE sequences of each snake species were aligned
478 to the consensus sequence to estimate their divergence level using RepeatMasker.

479 For gene annotation, we combined resources of sequence homology, *de novo*
480 prediction and transcriptome to build consensus gene models of the reference genome.
481 Protein sequences of green lizard, chicken and human were aligned to the reference
482 assembly using TBLASTN (E-value $\leq 1E-5$)⁶⁰. Then the candidate gene regions were
483 refined by GeneWise⁶¹ for more accurate splicing sites and gene models. We randomly
484 selected 1000 homology-based genes to train Augustus⁶² for *de novo* prediction on the
485 pre-masked genome sequences. We mapped RNA-seq reads of 13 samples to the genome
486 using TopHat (v1.3.1)⁶³ and then assembled the transcripts by Cufflinks (v1.3.0)
487 (<http://cufflinks.cbc.umd.edu/>). Transcripts from different samples were merged by
488 Cuffmerge. Finally, gene models from these three methods were combined into a
489 non-redundant gene set.

490 We finally obtained 21,194 protein-coding genes with intact open reading frames
491 (ORFs) (**Supplementary Table 14**). The gene models (measured by gene length, mRNA
492 length, exon number and exon length) are comparable to those of other vertebrates and
493 are well supported by the RNA-Seq data (**Supplementary Figure 18 and**
494 **Supplementary Table 5**). To annotate the gene names for each predicted protein-coding
495 locus, we first mapped all the 21,194 genes to a manually collected Ensembl gene library,
496 which consists of all proteins from *Anolis carolinensis*, *Gallus gallus*, *Homo sapiens*,

497 *Xenopus tropicalis* and *Danio rerio*. Then the best hit of each snake gene was retained
498 based on its BLAST alignment score, and the gene name of this best hit gene was
499 assigned to the query snake gene. Most of the predicted genes can be found for their
500 orthologous genes in the library at a threshold of 80% alignment rate (the aligned length
501 divided by the original protein length), suggesting our annotation has a high quality
502 **(Supplementary Table 15)**.

503

504 **RNA-seq and gene expression analyses**

505 Total RNAs were isolated from four types of tissues collected from both sexes, including
506 brain, liver, venom gland and gonad **(Supplementary Table 16)**. RNA sequencing
507 libraries were constructed using the Illumina mRNA-Seq Prep Kit. Briefly, oligo(dT)
508 magnetic beads were used to purify poly-A containing mRNA molecules. The mRNAs
509 were further fragmented and randomly primed during the first strand synthesis by reverse
510 transcription. This procedure was followed by a second-strand synthesis with DNA
511 polymerase I to create double-stranded cDNA fragments. The cDNAs were subjected to
512 end-repairing by Klenow and T4 DNA polymerases and A-tailed by Klenow lacking
513 exonuclease activity. The fragments were ligated to Illumina Paired-End Sequencing
514 adapters, size selected by gel electrophoresis and then PCR amplified to complete the
515 library preparation. The paired-end libraries were sequenced using Illumina HiSeq 2000
516 (90/100 bp at each end).

517 We used TopHat (v1.3.1) for aligning the RNA-seq reads and predicting the splicing
518 junctions with the following parameters: `-I/--max-intron-length: 10000, --segment-length:`
519 `25, --library-type: fr-firststrand, --mate-std-dev 10, -r/--mate-inner-dist: 20`. Gene
520 expression was measured by reads per kilobase of gene per million mapped reads
521 (RPKM). To minimize the influence of different samples, RPKMs were adjusted by a
522 scaling method based on TMM (trimmed mean of M values; M values mean the log
523 expression ratios)⁶⁴ which assumes that the majority of genes are common to all samples
524 and should not be differentially expressed.

525

526 Evolution analyses

527 A phylogenetic tree of the five-pacer viper and the other sequenced genomes (*Xenopus*
528 *tropicalis*, *Homo sapiens*, *Mus musculus*, *Gallus gallus*, *Chelonia mydas*, *Alligator*
529 *mississippiensis*, *Anolis carolinensis*, *Boa constrictor*, *Python bivittatus* and *Ophiophagus*
530 *hannah*) was constructed using the 5,353 orthologous single-copy genes. Treebest
531 (<http://treesoft.sourceforge.net/treebest.shtml>) was used to construct the phylogenetic tree.
532 To estimate the divergence times between species, for each species, 4-fold degenerate
533 sites were extracted from each orthologous family and concatenated to one sequence for
534 each species. The MCMCtree program implemented in the Phylogenetic Analysis by
535 Maximum Likelihood (PAML)⁶⁵ package was used to estimate the species divergence
536 time. Calibration time was obtained from the TimeTree database
537 (<http://www.timetree.org/>). Three calibration points were applied in this study as normal
538 priors to constrain the age of the nodes described below. 61.5-100.5 MA for the most
539 recent common ancestor (TMRCA) of human-mouse; 259.7-299.8 MA for TMRCA of
540 Crocodylidae and Lepidosauria; 235- 250.4 MA for TMRCA of Aves and Crocodylidae⁶⁶.

541 To examine the evolution of gene families in Squamate reptiles, genes from four
542 snakes (*Boa constrictor*, *Python bivittatus*, *Deinagkistrodon acutus*, *Ophiophagus*
543 *hannah*) and green anole lizard were clustered into gene families by Treefam
544 (min_weight=10, min_density=0.34, and max_size=500)⁶⁷. The family expansion or
545 contraction analysis was performed by CAFE⁶⁸. In CAFE, a random birth-and-death
546 model was proposed to study gene gain and loss in gene families across a user-specified
547 phylogenetic tree. A global parameter λ (lambda), which described both gene birth (λ)
548 and death ($\mu = -\lambda$) rate across all branches in the tree for all gene families was estimated
549 using maximum likelihood method. A conditional p-value was calculated for each gene
550 family, and the families with conditional p-values lower than 0.05 were considered to
551 have a significantly accelerated rate of expansion and contraction.

552 For the PAML analyses, we first assigned orthologous relationships for 12,657 gene
553 groups among all Squamata and outgroup (turtle) using the reciprocal best blast hit
554 algorithm and syntenic information. We used PRANK⁶⁹ to align the orthologous gene
555 sequences, which takes phylogenetic information into account when placing a gap into

556 the alignment. We filtered the PRANK alignments by gblocks⁷⁰ and excluded genes with
557 high proportion of low complexity or repetitive sequences to avoid alignment errors. To
558 identify the genes that evolve under positive selection (PSGs), we performed likelihood
559 ratio test (LRT) using the branch model by PAML⁶⁵. We first performed a LRT of the
560 two-ratio model, which calculates the dN/dS ratio for the lineage of interest and the
561 background lineage, against the one-ratio model assuming a uniform dN/dS ratio across all
562 branches, so that to determine whether the focal lineage is evolving significantly faster
563 (p-value < 0.05). In order to differentiate between episodes of positive selection and
564 relaxation of purifying selection (RSGs), we performed a LRT of two-ratios model
565 against the model that fixed the focal lineage's dN/dS ratio to be 1 (p-value < 0.05) and
566 also required PSGs with the free-ratio model dN/dS > 1 at the focal lineage. For the
567 identified RSGs and PSGs, we used their mouse orthologs' mutant phenotype
568 information⁷¹ and performed enrichment analyses using MamPhEA⁷². Then we grouped
569 the enriched MP terms by different tissue types.

570

571 **Olfactory receptor (OR), *Hox* and venom gene annotation**

572 To identify the nearly complete functional gene repertoire of OR, *Hox* and venom toxin
573 genes in the investigated species, we first collected known amino acid sequences of 458
574 intact OR genes from three species (green anole lizard, chicken and zebra finch)⁷³, all
575 annotated *Hox* genes from *Mus musculus* and *HoxC3* from *Xenopus tropicalis*, and
576 obtained the query sequences of a total of 35 venom gene families⁷⁴ from UniProt
577 (<http://www.uniprot.org/>) and NCBI (<http://www.ncbi.nlm.nih.gov/>). These 35 venom
578 gene families represent the vast majority of known snake venoms. Then we performed a
579 TBlastN⁶⁰ search with the cutoff E-value of 1E-5 against the genomic data using these
580 query sequences. Aligned sequence fragments were combined into one predicted gene
581 using perl scripts if they belonged to the same query protein. Then each candidate gene
582 region was extended for 2kb from both ends to predict its open reading frame by
583 GeneWise⁶¹. Obtained sequences were verified as corresponding genes by BlastP
584 searches against NCBI nonredundant (nr) database. Redundant annotations within
585 overlapped genomic regions were removed.

586 For the OR gene prediction, these candidates were classified into functional genes
587 and nonfunctional pseudogenes. If a sequence contained any disruptive frame-shift
588 mutations and/or premature stop codons, it was annotated as a pseudogene. The
589 remaining genes were examined using TMHMM2.0⁷⁵. Those OR genes containing more
590 at least 6 transmembrane (TM) structures were considered as intact candidates and the
591 rest were also considered as pseudogenes. Finally, each OR sequence identified was
592 searched against the HORDE (the Human Olfactory Data Explorer) database
593 (<http://genome.weizmann.ac.il/horde/>) using the FASTA (<ftp://ftp.virginia.edu/pub/fasta>)
594 and classified into the different families according to their best-aligned human OR
595 sequence. For the venom toxin genes, we only kept these genes with RPKM higher than 1
596 in the five-pacer viper and king cobra venom gland tissue as final toxin gene set.

597

598 **Identification and analyses of sex-linked genes**

599 To identify the Z-linked scaffolds in the male assembly, we aligned the female and male
600 reads to the male genome separately with BWA⁵⁸ allowing 2 mismatches and 1 indel.
601 Scaffolds with less than 80% alignment coverage (excluding gaps) or shorter than 500 bp
602 in length were excluded. Then single-base depths were calculated using SAMtools⁷⁶, with
603 which we calculated the coverage and mean depth for each scaffold. The expected male
604 vs. female (M:F) scaled ratio of a Z-linked scaffold is equal to 2, and we defined a
605 Z-linked scaffold with the variation of an observed scaled ratio to be less than 20% (i.e.
606 1.6 to 2.4). With this criteria, we identified 139 Z-lined scaffolds, representing 76.93Mb
607 with a scaffold N50 of 962 kb (**Supplementary Table 17**). These Z-linked scaffolds were
608 organized into pseudo-chromosome sequence based on their homology with green anole
609 lizard. Another characteristic pattern of the Z-linked scaffolds is that there should be
610 more heterozygous SNPs in the male individual than in the female individual resulted
611 from their hemizygous state in female. We used SAMtools⁷⁶ for SNP/indel calling. SNPs
612 and indels whose read depths were too low (<10) or too high (>120), or qualities lower
613 than 100 were excluded. As expected, the frequency of heterozygous sites of Z
614 chromosome of the female individual is much lower than that of the male individual
615 (0.005% vs 0.08%), while the heterozygous rate of autosomes are similar in both sex

616 (~0.1%) (**Supplementary Table 18**). To identify the W-linked scaffolds, we used the
617 similar strategy as the Z-linked scaffold detection to obtain the coverage and mean depth
618 of each scaffold. Then we identified those scaffolds covered by female reads over 80% of
619 the length, and by male reads with less than 20% of the length. With this method, we
620 identified 33 Mb W-linked scaffolds with a scaffold N50 of 48 kb (**Supplementary Table**
621 **19**).

622 We used the protein sequences of Z/W gametologs from garter snake and pygmy
623 rattle snake¹² as queries and aligned them to the genomes of boa (the SGA assembly,
624 <http://gigadb.org/dataset/100060>), five-pacer viper and king cobra with BLAST⁶⁰. The
625 best aligned (cutoff: identity \geq 70%, coverage \geq 50%) region with extended flanking
626 sequences of 5kb at both ends was then used to determine whether it contains an intact
627 open reading frame (ORF) by GeneWise⁶¹ (-tfor -genesf -gff -sum). We annotated the
628 ORF as disrupted when GeneWise reported at least one premature stop codon or
629 frame-shift mutation. CDS sequences of single-copy genes' Z/W gametologs were
630 aligned by MUSCLE⁷⁷ and the resulting alignments were cleaned by gblocks⁷⁰ (-b4=5,
631 -t=c, -e=-gb). Only alignments longer than 300bp were used for constructing maximum
632 likelihood trees by RAxML⁷⁸ to infer whether their residing evolutionary stratum is
633 shared among species or specific to lineages.

634

635 **Data availability**

636

637 **References**

- 638 1 Greene, H. W. *Snakes: the evolution of mystery in nature*. (Univ of California
639 Press, 1997).
- 640 2 Tchernov, E., Rieppel, O., Zaher, H., Polcyn, M. J. & Jacobs, L. L. A fossil snake
641 with limbs. *Science* **287**, 2010-2012 (2000).
- 642 3 Cohn, M. J. & Tickle, C. Developmental basis of limblessness and axial
643 patterning in snakes. *Nature* **399**, 474-479, doi:10.1038/20944 (1999).
- 644 4 Apesteguia, S. & Zaher, H. A Cretaceous terrestrial snake with robust hindlimbs
645 and a sacrum. *Nature* **440**, 1037-1040, doi:10.1038/nature04413 (2006).

- 646 5 Gracheva, E. O. *et al.* Molecular basis of infrared detection by snakes. *Nature* **464**,
647 1006-1011, doi:10.1038/nature08943 (2010).
- 648 6 Vonk, F. J. *et al.* Evolutionary origin and development of snake fangs. *Nature* **454**,
649 630-633, doi:10.1038/nature07178 (2008).
- 650 7 Di-Poi, N. *et al.* Changes in Hox genes' structure and function during the
651 evolution of the squamate body plan. *Nature* **464**, 99-103,
652 doi:10.1038/nature08789 (2010).
- 653 8 Guerreiro, I. *et al.* Role of a polymorphism in a Hox/Pax-responsive enhancer in
654 the evolution of the vertebrate spine. *Proc Natl Acad Sci U S A* **110**, 10682-10686,
655 doi:10.1073/pnas.1300592110 (2013).
- 656 9 Fry, B. G. From genome to "venome": molecular origin and evolution of the
657 snake venom proteome inferred from phylogenetic analysis of toxin sequences
658 and related body proteins. *Genome Res* **15**, 403-420, doi:10.1101/gr.3228405
659 (2005).
- 660 10 Vonk, F. J. *et al.* The king cobra genome reveals dynamic gene evolution and
661 adaptation in the snake venom system. *Proc Natl Acad Sci U S A* **110**,
662 20651-20656, doi:10.1073/pnas.1314702110 (2013).
- 663 11 Fry, B. G., Vidal, N., van der Weerd, L., Kochva, E. & Renjifo, C. Evolution and
664 diversification of the Toxicofera reptile venom system. *J Proteomics* **72**, 127-136,
665 doi:10.1016/j.jprot.2009.01.009 (2009).
- 666 12 Vicoso, B., Emerson, J. J., Zektser, Y., Mahajan, S. & Bachtrog, D. Comparative
667 sex chromosome genomics in snakes: differentiation, evolutionary strata, and lack
668 of global dosage compensation. *PLoS Biol* **11**, e1001643,
669 doi:10.1371/journal.pbio.1001643 (2013).
- 670 13 Ohno, S. *Sex Chromosomes and Sex-linked Genes*. Vol. 1967 (Springer Berlin
671 Heidelberg, 1967).
- 672 14 Kaiser, V. B. & Bachtrog, D. Evolution of sex chromosomes in insects. *Annu Rev*
673 *Genet* **44**, 91-112, doi:10.1146/annurev-genet-102209-163600 (2010).
- 674 15 Westergaard, M. The mechanism of sex determination in dioecious flowering
675 plants. *Adv Genet* **9**, 217-281 (1958).

- 676 16 Castoe, T. A. *et al.* The Burmese python genome reveals the molecular basis for
677 extreme adaptation in snakes. *Proc Natl Acad Sci U S A* **110**, 20645-20650,
678 doi:10.1073/pnas.1314475110 (2013).
- 679 17 Woltering, J. M. *et al.* Axial patterning in snakes and caecilians: evidence for an
680 alternative interpretation of the Hox code. *Dev Biol* **332**, 82-89,
681 doi:10.1016/j.ydbio.2009.04.031 (2009).
- 682 18 Head, J. J. & Polly, P. D. Evolution of the snake body form reveals homoplasmy in
683 amniote Hox gene function. *Nature* **520**, 86-89, doi:10.1038/nature14042 (2015).
- 684 19 Gomez, C. *et al.* Control of segment number in vertebrate embryos. *Nature* **454**,
685 335-339, doi:10.1038/nature07020 (2008).
- 686 20 Zhang, B. *et al.* Transcriptome analysis of *Deinagkistrodon acutus* venomous
687 gland focusing on cellular structure and functional aspects using expressed
688 sequence tags. *BMC Genomics* **7** (2006).
- 689 21 Bradnam, K. R. *et al.* Assemblathon 2: evaluating de novo methods of genome
690 assembly in three vertebrate species. *Gigascience* **2**, 10,
691 doi:10.1186/2047-217X-2-10 (2013).
- 692 22 Lin, X. *et al.* The effect of the fibrinolytic enzyme FIIa from *Agkistrodon acutus*
693 venom on acute pulmonary thromboembolism. *Acta Pharmacologica Sinica* **32**,
694 239-244 (2011).
- 695 23 Li, Z. *et al.* Comparison of the two major classes of assembly algorithms:
696 overlap-layout-consensus and de-bruijn-graph. *Brief Funct Genomics* **11**, 25-37,
697 doi:10.1093/bfgp/elr035 (2012).
- 698 24 Alfoldi, J. *et al.* The genome of the green anole lizard and a comparative analysis
699 with birds and mammals. *Nature* **477**, 587-591, doi:10.1038/nature10390 (2011).
- 700 25 Pyron, R. A. & Burbrink, F. T. Extinction, ecological opportunity, and the origins
701 of global snake diversity. *Evolution* **66**, 163-178,
702 doi:10.1111/j.1558-5646.2011.01437.x (2012).
- 703 26 Yunfang, Q., Xingfu, X., Youjin, Y., Fuming, D. & Meihua., H. Chromosomal
704 studies on six species of venomous snakes in Zhejiang. *Acta Zoologica Sinica* **273**,
705 218-227 (1981).

- 706 27 Srikulnath, K. *et al.* Karyotypic evolution in squamate reptiles: comparative gene
707 mapping revealed highly conserved linkage homology between the butterfly
708 lizard (*Leiolepis reevesii rubritaeniata*, Agamidae, Lacertilia) and the Japanese
709 four-striped rat snake (*Elaphe quadrivirgata*, Colubridae, Serpentes). *Chromosome*
710 *Res* **17**, 975-986, doi:10.1007/s10577-009-9101-7 (2009).
- 711 28 Yang, Z. Likelihood ratio tests for detecting positive selection and application to
712 primate lysozyme evolution. *Mol Biol Evol* **15**, 568-573 (1998).
- 713 29 Martill, D. M., Tischlinger, H. & Longrich, N. R. EVOLUTION. A four-legged
714 snake from the Early Cretaceous of Gondwana. *Science* **349**, 416-419,
715 doi:10.1126/science.aaa9208 (2015).
- 716 30 Held, J. *How the Snake Lost Its Legs: Curious Tales from the Frontier of*
717 *Evo-Devo.* (Cambridge University Press, 2014).
- 718 31 Xu, B. *et al.* Hox5 interacts with Plzf to restrict Shh expression in the developing
719 forelimb. *Proc Natl Acad Sci U S A* **110**, 19438-19443,
720 doi:10.1073/pnas.1315075110 (2013).
- 721 32 Boulet, A. M. & Capecchi, M. R. Multiple roles of Hoxa11 and Hoxd11 in the
722 formation of the mammalian forelimb zeugopod. *Development* **131**, 299-309,
723 doi:10.1242/dev.00936 (2004).
- 724 33 King, M., Arnold, J. S., Shanske, A. & Morrow, B. E. T-genes and limb bud
725 development. *Am J Med Genet A* **140**, 1407-1413, doi:10.1002/ajmg.a.31250
726 (2006).
- 727 34 Logan, M. & Tabin, C. J. Role of Pitx1 upstream of Tbx4 in specification of
728 hindlimb identity. *Science* **283**, 1736-1739 (1999).
- 729 35 Wellik, D. M. & Capecchi, M. R. Hox10 and Hox11 genes are required to
730 globally pattern the mammalian skeleton. *Science* **301**, 363-367,
731 doi:10.1126/science.1085672 (2003).
- 732 36 McGrew, M. J., Dale, J. K., Fraboulet, S. & Pourquie, O. The lunatic fringe gene
733 is a target of the molecular clock linked to somite segmentation in avian embryos.
734 *Curr Biol* **8**, 979-982 (1998).
- 735 37 Muragaki, Y., Mundlos, S., Upton, J. & Olsen, B. R. Altered growth and

- 736 branching patterns in synpolydactyly caused by mutations in HOXD13. *Science*
737 **272**, 548-551 (1996).
- 738 38 Kaske, S. *et al.* TRPM5, a taste-signaling transient receptor potential ion-channel,
739 is a ubiquitous signaling component in chemosensory cells. *BMC Neuroscience* **8**,
740 49 (2007).
- 741 39 Dehara, Y. *et al.* Characterization of squamate olfactory receptor genes and their
742 transcripts by the high-throughput sequencing approach. *Genome Biol Evol* **4**,
743 602-616, doi:10.1093/gbe/evs041 (2012).
- 744 40 Khan, I. *et al.* Olfactory receptor subgenomes linked with broad ecological
745 adaptations in Sauropsida. *Mol Biol Evol* **32**, 2832-2843,
746 doi:10.1093/molbev/msv155 (2015).
- 747 41 Hayden, S. *et al.* A cluster of olfactory receptor genes linked to frugivory in bats.
748 *Mol Biol Evol* **31**, 917-927, doi:10.1093/molbev/msu043 (2014).
- 749 42 Daltry, J. C., Wuster, W. & Thorpe, R. S. Diet and snake venom evolution. *Nature*
750 **379**, 537-540, doi:10.1038/379537a0 (1996).
- 751 43 Hargreaves, A. D., Swain, M. T., Hegarty, M. J., Logan, D. W. & Mulley, J. F.
752 Restriction and recruitment-gene duplication and the origin and evolution of
753 snake venom toxins. *Genome Biol Evol* **6**, 2088-2095, doi:10.1093/gbe/evu166
754 (2014).
- 755 44 Casewell, N. R., Harrison, R. A., Wuster, W. & Wagstaff, S. C. Comparative
756 venom gland transcriptome surveys of the saw-scaled vipers (Viperidae: Echis)
757 reveal substantial intra-family gene diversity and novel venom transcripts. *BMC*
758 *Genomics* **10**, 564, doi:10.1186/1471-2164-10-564 (2009).
- 759 45 Matsubara, K. *et al.* Evidence for different origin of sex chromosomes in snakes,
760 birds, and mammals and step-wise differentiation of snake sex chromosomes.
761 *Proc Natl Acad Sci U S A* **103**, 18190-18195, doi:10.1073/pnas.0605274103
762 (2006).
- 763 46 Ohno, S. *Sex chromosomes and sex-linked genes*. Vol. 1 (Springer, 1967).
- 764 47 Zhou, Q. *et al.* Complex evolutionary trajectories of sex chromosomes across bird
765 taxa. *Science* **346**, 1246338, doi:10.1126/science.1246338 (2014).

- 766 48 Cortez, D. *et al.* Origins and functional evolution of Y chromosomes across
767 mammals. *Nature* **508**, 488-493, doi:10.1038/nature13151 (2014).
- 768 49 Nicolas, M. *et al.* A gradual process of recombination restriction in the
769 evolutionary history of the sex chromosomes in dioecious plants. *PLoS Biol* **3**, e4,
770 doi:10.1371/journal.pbio.0030004 (2005).
- 771 50 Li, W. H., Yi, S. & Makova, K. Male-driven evolution. *Curr Opin Genet Dev* **12**,
772 650-656 (2002).
- 773 51 Vicoso, B. & Charlesworth, B. Evolution on the X chromosome: unusual patterns
774 and processes. *Nat Rev Genet* **7**, 645-653, doi:10.1038/nrg1914 (2006).
- 775 52 Mank, J. E. The W, X, Y and Z of sex-chromosome dosage compensation. *Trends*
776 *Genet* **25**, 226-233, doi:10.1016/j.tig.2009.03.005 (2009).
- 777 53 Boucherat, O. *et al.* Partial functional redundancy between Hoxa5 and Hoxb5
778 paralog genes during lung morphogenesis. *Am J Physiol Lung Cell Mol Physiol*
779 **304**, L817-L830 (2013).
- 780 54 Guerreiro, I. & Duboule, D. Snakes: hatching of a model system for Evo-Devo?
781 *Int J Dev Biol* **58**, 727-732, doi:10.1387/ijdb.150026dd (2014).
- 782 55 Booth, W., Johnson, D. H., Moore, S., Schal, C. & Vargo, E. L. Evidence for
783 viable, non-clonal but fatherless Boa constrictors. *Biol Lett* **7**, 253-256,
784 doi:10.1098/rsbl.2010.0793 (2011).
- 785 56 Li, R. *et al.* The sequence and de novo assembly of the giant panda genome.
786 *Nature* **463**, 311-317, doi:10.1038/nature08696 (2010).
- 787 57 Luo, R. *et al.* SOAPdenovo2: an empirically improved memory-efficient
788 short-read de novo assembler. *Gigascience* **1**, 18, doi:10.1186/2047-217X-1-18
789 (2012).
- 790 58 Li, H. & Durbin, R. Fast and accurate short read alignment with Burrows-Wheeler
791 transform. *Bioinformatics* **25**, 1754-1760, doi:10.1093/bioinformatics/btp324
792 (2009).
- 793 59 Jurka, J. Repbase update: a database and an electronic journal of repetitive
794 elements. *Trends Genet* **16**, 418-420 (2000).
- 795 60 Altschul, S. F., Gish, W., Miller, W., Myers, E. W. & Lipman, D. J. Basic local

- 796 alignment search tool. *J Mol Biol* **215**, 403-410,
797 doi:10.1016/S0022-2836(05)80360-2 (1990).
- 798 61 Birney, E., Clamp, M. & Durbin, R. GeneWise and Genomewise. *Genome Res* **14**,
799 988-995, doi:10.1101/gr.1865504 (2004).
- 800 62 Stanke, M., Steinkamp, R., Waack, S. & Morgenstern, B. AUGUSTUS: a web
801 server for gene finding in eukaryotes. *Nucleic Acids Res* **32**, W309-312,
802 doi:10.1093/nar/gkh379 (2004).
- 803 63 Trapnell, C., Pachter, L. & Salzberg, S. L. TopHat: discovering splice junctions
804 with RNA-Seq. *Bioinformatics* **25**, 1105-1111, doi:10.1093/bioinformatics/btp120
805 (2009).
- 806 64 Robinson, M. D. & Oshlack, A. A scaling normalization method for differential
807 expression analysis of RNA-seq data. *Genome Biol* **11**, R25,
808 doi:10.1186/gb-2010-11-3-r25 (2010).
- 809 65 Yang, Z. PAML 4: phylogenetic analysis by maximum likelihood. *Mol Biol Evol*
810 **24**, 1586-1591, doi:10.1093/molbev/msm088 (2007).
- 811 66 Benton, M. J. & Donoghue, P. C. Paleontological evidence to date the tree of life.
812 *Mol Biol Evol* **24**, 26-53, doi:10.1093/molbev/msl150 (2007).
- 813 67 Li, H. *et al.* TreeFam: a curated database of phylogenetic trees of animal gene
814 families. *Nucleic Acids Res* **34**, D572-580, doi:10.1093/nar/gkj118 (2006).
- 815 68 De Bie, T., Cristianini, N., Demuth, J. P. & Hahn, M. W. CAFE: a computational
816 tool for the study of gene family evolution. *Bioinformatics* **22**, 1269-1271,
817 doi:10.1093/bioinformatics/btl097 (2006).
- 818 69 Loytynoja, A. & Goldman, N. An algorithm for progressive multiple alignment of
819 sequences with insertions. *Proc Natl Acad Sci U S A* **102**, 10557-10562,
820 doi:10.1073/pnas.0409137102 (2005).
- 821 70 Talavera, G. & Castresana, J. Improvement of phylogenies after removing
822 divergent and ambiguously aligned blocks from protein sequence alignments. *Syst*
823 *Biol* **56**, 564-577, doi:10.1080/10635150701472164 (2007).
- 824 71 Bult, C. J. *et al.* Mouse genome database 2016. *Nucleic Acids Res* **44**, D840-847,
825 doi:10.1093/nar/gkv1211 (2016).

- 826 72 Weng, M. P. & Liao, B. Y. MamPhEA: a web tool for mammalian phenotype
827 enrichment analysis. *Bioinformatics* **26**, 2212-2213,
828 doi:10.1093/bioinformatics/btq359 (2010).
- 829 73 Steiger, S. S., Kuryshev, V. Y., Stensmyr, M. C., Kempnaers, B. & Mueller, J. C.
830 A comparison of reptilian and avian olfactory receptor gene repertoires:
831 species-specific expansion of group gamma genes in birds. *BMC Genomics* **10**,
832 446, doi:10.1186/1471-2164-10-446 (2009).
- 833 74 Mackessy, S. P. *Handbook of venoms and toxins of reptiles*. (CRC Press, 2016).
- 834 75 Krogh, A., Larsson, B., von Heijne, G. & Sonnhammer, E. L. Predicting
835 transmembrane protein topology with a hidden Markov model: application to
836 complete genomes. *J Mol Biol* **305**, 567-580, doi:10.1006/jmbi.2000.4315 (2001).
- 837 76 Li, H. *et al.* The Sequence Alignment/Map format and SAMtools. *Bioinformatics*
838 **25**, 2078-2079, doi:10.1093/bioinformatics/btp352 (2009).
- 839 77 Edgar, R. C. MUSCLE: multiple sequence alignment with high accuracy and high
840 throughput. *Nucleic Acids Res* **32**, 1792-1797, doi:10.1093/nar/gkh340 (2004).
- 841 78 Stamatakis, A. RAxML version 8: a tool for phylogenetic analysis and
842 post-analysis of large phylogenies. *Bioinformatics* **30**, 1312-1313,
843 doi:10.1093/bioinformatics/btu033 (2014).
- 844

845 **Acknowledgements**

846 This project was supported by the Thousand Young Talents Program funding, and a
847 startup funding of Life Science Institute of Zhejiang University to Q. Z., and National
848 Major Scientific and Technological Special Project for ‘Significant New Drugs
849 Development’ during the Twelfth Five-year Plan Period (No. 2009ZX09102-217,
850 2009-2010) to W. Y. All the raw reads, genome assembly and annotation generated in
851 this study are deposited under the BioProject # PRJNA314370 on NCBI.

852

853 **Author Contributions**

854 Q.Z., W.Y., G.Y. conceived and supervised the project. B.L., P.Q., W.Z., Y.H. and X.S.
855 provided and extracted the samples. Z.L. and B.W. performed the proteomic mass
856 spectrometry-based experiment and data analysis. J.L., Z.W. and Y.Z. performed the
857 genome assembly and annotation. J.L. and Q.L. designed and performed the
858 identification of sex-linked scaffolds. P.Z. performed RNA-seq data analysis. Z.W., L.J.
859 and Y.Z. performed the genome evolution analyses. Z.W., Y.Z., L.J. and B.Q. performed
860 genes and gene family evolution analyses. Z.W. and L.J. performed the sex chromosome
861 evolution analyses. Q.Z., Z.W., G.Z., G.Y. interpreted the results and wrote the
862 manuscript. All of the authors read and approved the final manuscript.

863

864 **Competing financial interests**

865 The authors declare no competing financial interests.

866

867 **Figure Legends**

868 **Figure 1.** The comparative genomic landscape of five-pacer viper

869 (A) *Deinagkistrodon acutus* (five-pacer viper) and eight adult tissues used in this study.

870 (B) Circos plot showing the linkage group assignment using lizard chromosomes as
871 reference (outmost circle), normalized female vs. male mapped read coverage ratio (blue
872 line) and GC-isochore structures of five-pacer viper (red), boa (yellow) and green anole
873 lizard (green). Both snake genomes have a much higher variation of local GC content
874 than that of green anole lizard. (C) Phylogenomic tree constructed using fourfold

875 degenerate sites from 8006 single-copy orthologous genes. We also showed bootstrapping
876 percentages, the numbers of inferred gene family expansion (in green) and contraction
877 (red), and corresponding phylogenetic terms at each node. MRCA: most recent common
878 ancestor.

879

880 **Figure 2.** Genomic and transcriptomic variation of snake transposable elements

881 **(A)** Violin plots showing each type of TE's frequency distribution of sequence divergence
882 level from the inferred ancestral consensus sequences. Clustering of TEs with similar
883 divergence levels, manifested as the 'bout' of the violin, corresponds to the burst of TE
884 amplification. **(B)** Bar plots comparing the genome-wide TE content between four snake
885 species. TE families were annotated combining information of sequence homology and
886 *de novo* prediction. **(C)** TE's average normalized expression level (measured by RPKM)
887 across different tissues in five-pace viper.

888

889 **Figure 3.** Evolution of snake genes and gene families

890 **(A)** Phylogenetic distribution of mutant phenotypes (MP) of mouse orthologs of snakes.
891 Each MP term is shown by an organ icon, and significantly enriched for snake genes
892 undergoing positive selection (red) or relaxed selective constraints (gray) inferred by
893 lineage-specific PAML analyses. **(B)** We show the four *Hox* gene clusters of snakes,
894 with each box showing the ratio of nonsynonymous (dN) over synonymous substitution
895 (dS) rate at the snake ancestor lineage. White boxes represent genes that haven't been
896 calculated for their ratios due to the genome assembly issue in species other than
897 five-pacer viper. Boxes with dotted line refer to genes with dS approaching 0, therefore
898 the dN/dS ratio cannot be directly shown. Each cluster contains up to 13 *Hox* genes with
899 some of them lost during evolution. We also marked certain *Hox* genes undergoing
900 positive selection (in red) or relaxed selective constraints (in green) at a specific lineage
901 above the box. Each lineage was denoted as: S: *Serpentes* (ancestor of all snakes), H:
902 *Henophidia* (ancestor of boa and python), B: *Boa constrictor*, P: *Python bivittatus*, C:
903 *Colubroidea*, D: *Deinagkistrodon acutus*, O: *Ophiophagus hannah*. **(C)** Comparing
904 olfactory receptor (OR) gene repertoire between boa, viper and lizard. Each cell

905 corresponds to a certain OR family (shown at y-axis) gene number on a certain
906 chromosome (x-axis). (D) Pie chart shows the composition of normalized venom gland
907 transcripts of male five-pacer viper. The heatmap shows the normalized expression level
908 (in RPKM) across different tissues of viper and king cobra. We grouped the venom genes
909 by their time of origination, shown at the bottom x-axis.

910

911 **Figure 4.** Snake sex chromosomes have at least three evolution strata

912 The three tracks in the top panel shows female read depths along the Z chromosome
913 relative to the median depth value of autosomes, Z/W pairwise sequence divergence
914 within intergenic regions, and female read depths of W-linked sequence fragments
915 relative to the median depth value of autosomes. Depths close to 1 suggest that the region
916 is a recombining pseudoautosomal region (PAR), whereas depths of 0.5 are expected in a
917 highly differentiated fully sex-linked region where females are hemizygous. The
918 identifiable W-linked fragments are much denser at the region 56Mb~70Mb, probably
919 because this region (denoted as stratum 3, S3) has suppressed recombination most
920 recently. S2 and S1 were identified and demarcated by characterizing the sequence
921 conservation level (measured by LASTZ alignment score, blue line) between the chrZs of
922 boa and viper. At the oldest stratum S1 where recombination has been suppressed for the
923 longest time, there is an enrichment of repetitive elements on the affected Z-linked region
924 (Gypsy track in red, 100kb non-overlapping sliding window). And these Z-linked TEs A
925 similar pattern was found in homologous recombining region of boa, but not in lizard.

926

927 **Supplementary Figure Legend**

928 **Supplementary Figure 1.** K-mer estimation of the genome size of five-pacer viper.

929 Distribution of 17-mer frequency in the used sequencing reads from female (left) and
930 male (right) samples. The x-axis represents the sequencing depth. The Y-axis represents
931 the proportion of a K-mer counts in total K-mer counts at a given sequencing depth. The
932 estimated genome size is about 1.43 Gb.

933

934 **Supplementary Figure 2.** GC isochore structure of different tetrapod genomes.

935 We show the standard deviation (SD) of GC content calculated with different window
936 size (3 kb to 320 kb) for different vertebrate genomes.

937

938 **Supplementary Figure 3.** Comparing expression levels of genes nearby expressed TEs
939 in each tissue.

940 We show expression patterns of genes around highly expressed TE (RPKM > 5) in
941 different tissues from both sexes, including brain, liver, venom gland and gonad. We also
942 performed comparison between the focal tissue vs. the other tissues. We show levels of
943 significance with asterisks. *: $0.001 \leq P\text{-value} < 0.01$; **: $0.0001 \leq P < 0.001$; ***:
944 $P < 0.0001$.

945

946 **Supplementary Figure 4.** Comparison of *Hox* gene structure between snakes and lizard.
947 Schematic representation of four *Hox* clusters in anole lizard, boa, Burmese python,
948 five-pacer viper and king cobra. Each number from 1 to 13 denotes the specific *Hox* gene
949 belonging to one cluster. We showed the length difference between each species vs.
950 mouse by the colored lines (for intergenic regions) or boxes (for intronic regions): a
951 1.5~3 fold increase of length was shown by blue, a more than 3-fold increase was shown
952 in red. Exons were shown by vertical lines, and dotted lines refer to exons with unknown
953 boundaries, either due to assembly issues. Double-slashes refer to the gap between two
954 different scaffolds.

955

956 **Supplementary Figure 5.** Repeat accumulation at *Hox* gene clusters.

957 Comparison of the TE and simple repeat content of *Hox* cluster genes with 5kb flanking
958 regions between snakes and lizard. We calculated the repeat density by dividing the total
959 length of specific repeat sequence vs. the length of corresponding region. This density was
960 normalized over the genome-wide repeat density and then shown by heatmap.

961

962 **Supplementary Figure 6.** Phylogenetic distribution of enriched MP terms.

963 We identified enriched mutant phenotypes (MP) of mouse orthologs of snake genes that
964 are undergoing lineage-specific positive selection (red) and relaxed selective constraints
965 (gray). And then we mapped these MP terms onto the snake phylogeny.

966

967 **Supplementary Figure 7.** Read coverage density plot of different linkage groups.

968 For each linkage group (from left to right, chrW, chrZ, chr1), male reads were plotted in
969 blue, and female reads in red. The identified chrW scaffolds in this work all show a
970 female-specific read depth pattern.

971

972 **Supplementary Figure 8.** Male-driven evolution effect in snakes.

973 For each gene, we calculated the substitution rates between anole lizard and each of boa,
974 Burmese python, five-pacer viper and king cobra at synonymous sites (dS) and
975 non-synonymous sites (dN) divided into different chromosome sets. To detect
976 branch-specific differences, we obtained for each gene the ratios of these evolutionary
977 rates between the different snake species vs. boa. Since boa's homologous chromosomal
978 region to the Z chromosomes of other advanced snakes represent the ancestral status of
979 snake sex chromosomes, a higher relative ratios of Z-linked dS of advanced snakes vs.
980 boa than those of autosomes indicate the male-driven evolution effect. We shown the
981 Wilcoxon test significant differences between the Z chromosome and the autosomes
982 (chr1-5) are marked with asterisks (***, P -value < 0.001).

983

984 **Supplementary Figure 9.** Repeat accumulation along the snake sex chromosomes.

985 Shown are comparisons of the distribution of Gypsy, CR1 and L1 content along the
986 chromosome in anole lizard, Boa and five-pacer viper. The TE content was calculated by
987 averaging the TE density of each sliding window of 100kb as well as the flanking 10
988 windows.

989

990 **Supplementary Figure 10.** Gene trees for Z and W linked gametologs in S1 region.

991 Shown are maximum likelihood (ML) trees using coding regions of Z and W allelic
992 sequences from multiple snake species, with the gene name under each tree and

993 bootstrapping values at each node. Trees that show separate clustering of Z- or W- linked
994 gametologs provide strong evidence that these genes suppressed recombination before the
995 speciation.

996

997 **Supplementary Figure 11.** Gene trees for Z and W linked gametologs in S2 region.

998

999 **Supplementary Figure 12.** Gene trees for Z and W linked gametologs in S3 region.

1000

1001 **Supplementary Figure 13.** Comparison of repeat content between viper chrZ and chrW.

1002 TE families were determined based on the combined annotations of Repbase,

1003 RepeatModeler, and coverage in the genome was annotated using in-house scripts.

1004

1005 **Supplementary Figure 14.** Comparison of gene expression across different

1006 chromosomes.

1007 We show gene expression patterns between different chromosome sets across tissues.

1008 ‘pseudo-W’ refers to W-linked genes that have premature stop codons or frameshift

1009 mutations

1010

1011 **Supplementary Figure 15.** Pairwise comparison of gene expression levels between

1012 homologous Z and W alleles.

1013

1014 **Supplementary Figure 16.** Gene expression along the Z chromosome and autosome

1015 chr5 in different tissues of five-pacer viper.

1016 We show log-based male-to-female gene expression ratio along the Z chromosomes and

1017 autosome chr5. Only genes with RPKM ≥ 1 in both the male and female were

1018 considered. If genes are mostly non-biased, the line is expected to centered at 0. The

1019 pattern indicates five-pacer viper lacks chromosome-wide dosage compensation.

1020

1021 **Supplementary Figure 17.** Frequency distribution of sequencing depth.

1022 Distribution of sequencing depth of the assembled female (left) and male (right) genomes

1023 by reads from the female and male samples. The peak depth is 76X and 77X for the
1024 female and male reads aligned to corresponding assembly, respectively.

1025

1026 **Supplementary Figure 18.** Comparisons of gene parameters among the sequenced
1027 representative species.

1028 We used the published genomes of *Gallus gallus*, *Homo sapiens*, *Anolis carolinensis*,
1029 *Boa constrictor* to compare with *Deinagkistrodon acutus*, without finding any obvious
1030 differences between them and five-pacer viper in the annotated genes' length and number.
1031 This indicates the high quality of gene annotation.

1032

1033 **Supplementary Table Legend**

1034 **Supplementary Table 1.** Statistics of five-pacer viper genome sequencing.

1035

1036 **Supplementary Table 2.** Statistics of 17-mer analysis.

1037

1038 **Supplementary Table 3.** Statistics of reads of small-insert and large-insert libraries
1039 aligned to the male assembly.
1040 *PE mapped* refer to reads being mapped to the genome as read pairs, and *SE mapped*
1041 represent reads being mapped to the genome as single reads.

1042

1043 **Supplementary Table 4.** Summary of the five-pacer viper genome assemblies.

1044

1045 **Supplementary Table 5.** Number of expressed genes of five-pacer viper.

1046

1047 **Supplementary Table 6.** Number of genes and scaffold size organized into
1048 chromosomes.

1049

1050 **Supplementary Table 7.** Comparison of repeat content between snakes and lizard.

1051

1052 **Supplementary Table 8.** Comparison of genome assembly quality between snakes and
1053 lizard.

1054

1055 **Supplementary Table 9.** Evolution of candidate limb-patterning genes in snakes.

1056 Candidate limb-patterning genes were collected from MGI database and published paper.
1057 Genes undergoing positive selection (P) or relaxed selective constraints (R), were
1058 identified by PAML analyses. N: there is no significant selection signal. ‘-‘ refers to
1059 genes that cannot be completely assembled for their coding sequences due to genome
1060 assembly gaps.

1061

1062 **Supplementary Table 10. Comparison of venom genes between snakes.**

1063 Statistics of venom gene families in the four snakes and anole lizard genomes based on
1064 homology-based prediction. AVIT: Prokineticin; C3: complement C3; CVF: Cobra
1065 Venom Factor; CRISPs: Cysteine-Rich Secretory Proteins; Hy: Hyaluronidases;
1066 Natriuretic: Natriuretic peptide; NGF: Snake Venom Nerve Growth Factors; PLA2-2A:
1067 Snake Venom Phospholipase A2 (type IIA); SVMP: Snake Venom Metalloproteinases;
1068 TL: thrombin-like snake venom serine proteinases; LAAO: Snake Venom L-Amino Acid
1069 Oxidases; PDE: phosphodiesterases; CLPs: snake C-type lectin-like proteins; VEGF:
1070 vascular endothelin growth factor; PLA2-1B: Snake Venom Phospholipase A2 (type IB);
1071 3FTX: The three-finger toxins; ACeH: Acetylcholinesterase;

1072

1073 **Supplementary Table 11. Comparison of repeat content between snake sex**

1074 chromosomes and their lizard homolog.

1075

1076 **Supplementary Table 12. Location of W-linked putative pseudogenes.**

1077

1078 **Supplementary Table 13. Fractions of bases covered by reads in the male assembly.**

1079

1080 **Supplementary Table 14. Characteristics of predicted protein-coding genes in the male**
1081 assembly.

1082

1083 **Supplementary Table 15. Number of predicted genes that can find homologs in the**
1084 Ensembl library with different aligning rate cutoff.

1085 Alignment rate was calculated by dividing the aligned length vs. the original protein
1086 length. And we required both the query and subject to satisfy our alignment cutoff. The
1087 Ensembl library consists of all proteins from *Anolis carolinensis*, *Gallus gallus*, *Homo*

1088 sapiens, *Xenopus tropicalis* and *Danio rerio*.

1089

1090 **Supplementary Table 16.** Data production and alignment statistic of RNA-Seq aligned

1091 to male genome assembly.

1092

1093 **Supplementary Table 17.** Statistics of the identified Z-linked scaffolds.

1094

1095 **Supplementary Table 18.** Statistics of SNPs identified in the female and male

1096 individual.

1097

1098 **Supplementary Table 19.** Statistics of identified W-linked scaffolds.

1099

1100 **Supplementary Data Legend**

1101 **Supplementary Data 1**

1102 Comparing five-pacer viper's chromosomal assignment vs. reported fluorescence in situ

1103 hybridization results.

1104

1105 **Supplementary Data 2**

1106 GO enrichment of nearby genes of TE highly expressed in brain.

1107

1108 **Supplementary Data 3**

1109 Positively selected genes (PSGs) and genes with relaxed selective constraints (RSGs) and

1110 their affected lineage.

1111

1112 **Supplementary Data 4**

1113 Mouse mutant terms' enrichment analyses of PSGs and RSGs across different snake

1114 branches.

1115

1116 **Supplementary Data 5**

1117 GO enrichment of expanded and contracted gene families across different snake lineages.

1118

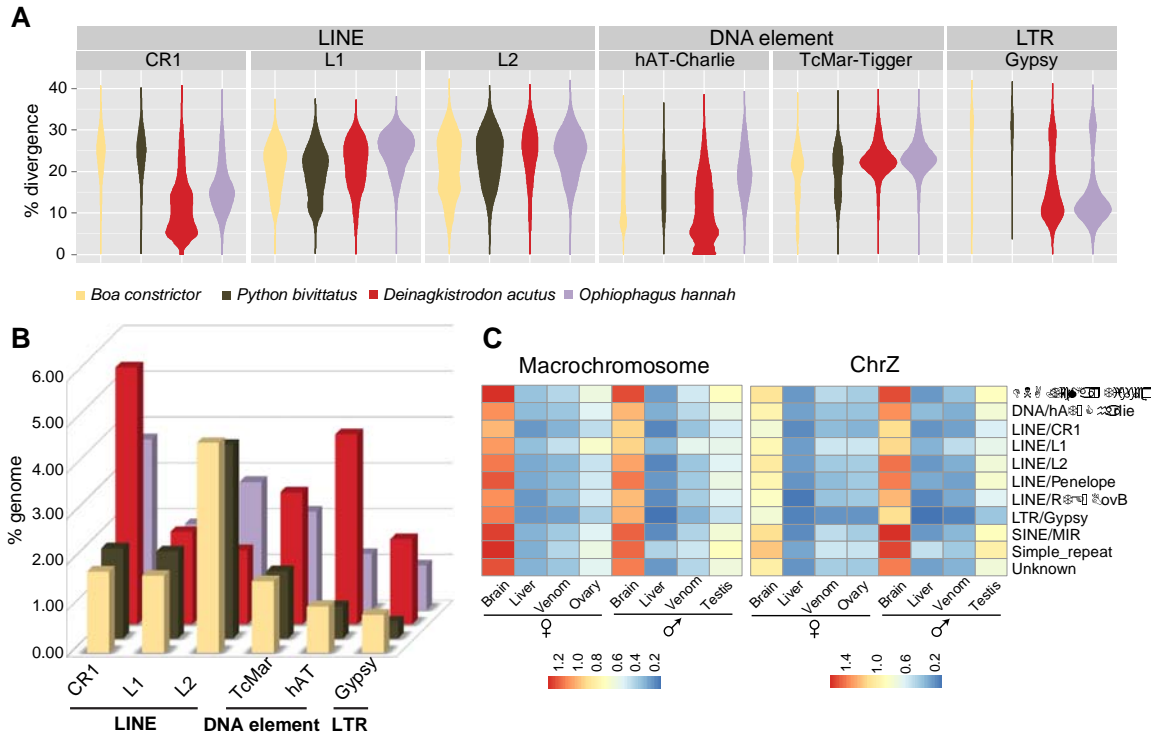
1119 **Supplementary Data 6**

1120 Plots of GO enrichment of expanded and contracted gene families using Ontologizer.

1121

1122

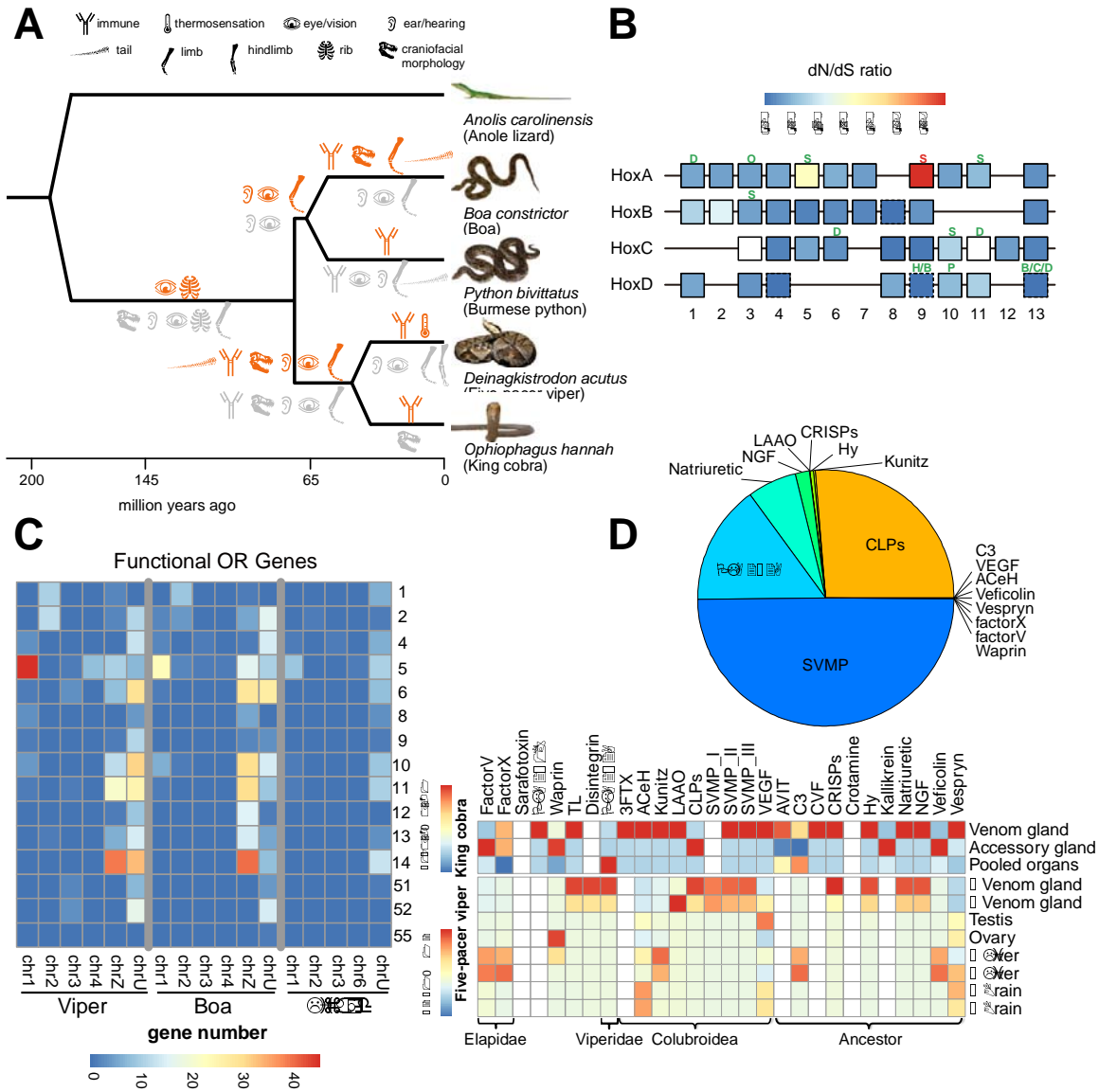
1126 **Figure 2.** Genomic and transcriptomic variation of snake transposable elements



1127

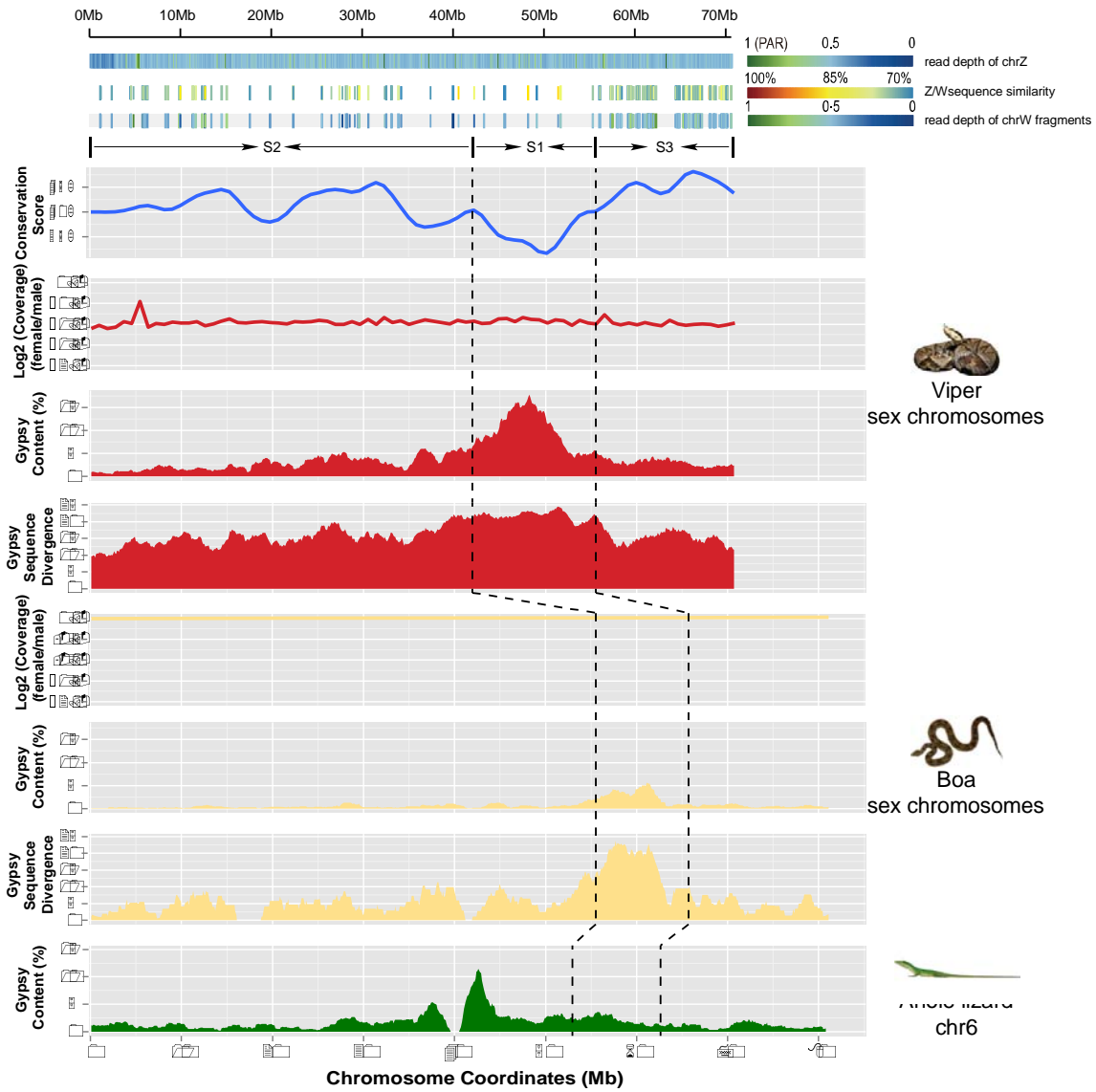
1128

1129 **Figure 3. Evolution of snake genes and gene families**



1130

1131 **Figure 4.** Snake sex chromosomes have at least three evolution strata



1132